frontiers in Molecular Biosciences

ORIGINAL RESEARCH
published: 25 July 2017
doi: 10.3389/fmolb.2017.00051

Metabolomics and Proteomics of *Brassica napus* Guard Cells in Response to Low CO_2

Sisi Geng[1,2], *Bing Yu*[2,3,4], *Ning Zhu*[2,5], *Craig Dufresne*[6] *and Sixue Chen*[1,2,5]*

[1] Plant Molecular and Cellular Biology Program, University of Florida, Gainesville, FL, United States, [2] Department of Biology, Genetics Institute, University of Florida, Gainesville, FL, United States, [3] Key Laboratory of Molecular Biology of Heilongjiang Province, College of Life Sciences, Heilongjiang University, Harbin, China, [4] Engineering Research Center of Agricultural Microbiology Technology, Ministry of Education, Heilongjiang University, Harbin, China, [5] Proteomics and Mass Spectrometry, Interdisciplinary Center for Biotechnology Research, University of Florida, Gainesville, FL, United States, [6] Thermo Fisher Scientific, West Palm Beach, FL, United States

Stomatal guard cell response to various stimuli is an important process that balances plant carbon dioxide (CO_2) uptake and water transpiration. Elevated CO_2 induces stomatal closure, while low CO_2 promotes stomatal opening. The signaling process of elevated CO_2 induced stomatal closure has been extensively studied in recent years. However, the mechanism of low CO_2 induced stomatal opening is not fully understood. Here we report metabolomic and proteomic responses of *Brassica napus* guard cells to low CO_2 using hyphenated mass spectrometry technologies. A total of 411 metabolites and 1397 proteins were quantified in a time-course study of low CO_2 effects. Metabolites and proteins that exhibited significant changes are overrepresented in fatty acid metabolism, starch and sucrose metabolism, glycolysis and redox regulation. Concomitantly, multiple hormones that promote stomatal opening increased in response to low CO_2. Interestingly, jasmonic acid precursors were diverted to a branch pathway of traumatic acid biosynthesis. These results indicate that the low CO_2 response is mediated by a complex crosstalk between different phytohormones.

Keywords: metabolomics, proteomics, *Brassica napus*, guard cells, low CO_2, phytohormone

OPEN ACCESS

Edited by:
Robert David Hall,
Wageningen University and Research Centre, Netherlands

Reviewed by:
Adam James Carroll,
Australian National University, Australia
Lena Fragner,
University of Vienna, Austria

***Correspondence:**
Sixue Chen
schen@ufl.edu

Specialty section:
This article was submitted to Metabolomics, a section of the journal Frontiers in Molecular Biosciences

Received: *20 February 2017*
Accepted: *06 July 2017*
Published: *25 July 2017*

Citation:
Geng S, Yu B, Zhu N, Dufresne C and Chen S (2017) Metabolomics and Proteomics of Brassica napus Guard Cells in Response to Low CO_2. Front. Mol. Biosci. 4:51. doi: 10.3389/fmolb.2017.00051

INTRODUCTION

Guard cells are specialized pairs of cells forming stomata, the tiny pores on leaf surfaces. Stomatal movement in response to various environmental signals as well as endogenous phytohormones such as abscisic acid (ABA) controls the balance of water transpiration and CO_2 intake for photosynthesis. It plays an essential role for plants to respond and adapt to their changing environmental conditions. An elevation of either intercellular CO_2 concentration (C_i) or atmospheric CO_2 concentration (C_a) can induce the closure of stomata (Engineer et al., 2015). In contrast, a decrease of CO_2 concentration will induce the opening of stomata (Negi et al., 2014). Atmospheric CO_2 has been increasing (at an average rate of about 2.1 ppm per year in the past 10 years (https://www.esrl.noaa.gov/gmd/ccgg/trends/gr.html). In spite of the overall increasing trend, diurnal and periodic decreases in CO_2 concentration have been observed (Zhu and Yoshikawa-Inoue, 2015). A better understanding of how plants respond to CO_2 changes is important for us to enhance crop production under the changing environment. The signaling pathway for elevated CO_2 induced stomatal closure shares many elements with the well-studied ABA signaling pathway

in guard cells, including the activation of OPEN STOMATA1 (OST1) and its target SLOW-TYPE ANION CHANNEL 1 (SLAC1) (Xue et al., 2011), reactive oxygen species (ROS) and nitric oxide (NO) production (Shi et al., 2015), and increase of cytosolic Ca^{2+} concentration (Schwartz et al., 1988; Webb et al., 1996). However, the high CO_2 signaling pathway has its unique components and does not completely overlap with the ABA signaling pathway. For example, several Arabidopsis mutants that are specifically insensitive to elevated CO_2 have been identified, including carbonic anhydrase double mutant *ca1ca4* (Hu et al., 2010), *rhc1* (*resistant to high $CO_2$1*) (Tian et al., 2015) and *ht1* (*high temperature 1*) (Tian et al., 2015). A comprehensive review on elevated CO_2 signaling in guard cells has been published recently (Engineer et al., 2015). Briefly, the signaling pathway starts with the conversion of CO_2 to bicarbonate by the activity of carbonic anhydrase (CA) 1 and CA4. The increased bicarbonate concentration in cytosol activates RHC1, which suppresses HT1, a negative regulator for high CO_2 induced stomatal closure. The inhibition of HT1 relieves OST1, which activates SLAC1 and facilitates stomatal closure by transporting Cl^- from cytosol to the intercellular space (Tian et al., 2015). OST1 also activates respiratory burst oxidase homolog (RBOH) D/F, which leads to ROS burst in the cytosol. Nitric oxide (NO) production is known to be downstream of ROS, and both H_2O_2 and NO can activate the tonoplast Ca^{2+} channel to trigger the release of Ca^{2+} into the cytosol. The increase in cytosol Ca^{2+} is an important step for CO_2 induced stomatal closure (Webb et al., 1996; Young et al., 2006; Xue et al., 2011). A rapid type anion channel responsible for $malate^{2-}$ export is also important in high CO_2 induced stomatal closure (Meyer et al., 2010). Another malate transporter (AtABCB14), which mediates malate import from intercellular space, has been shown to be a negative regulator for high CO_2 induced stomatal closure (Lee et al., 2008). In our previous study, we observed increases of jasmonic acids (JAs) in guard cells under high CO_2. The increase was not observed in the *ca1ca4* mutant, JA biosynthesis and signaling mutants, which exhibited impaired high CO_2 responses (Geng et al., 2016). These results indicate a potential role of JA in high CO_2 induced stomatal closure.

Despite significant progress made in guard cell elevated CO_2 response, the mechanisms for low CO_2 induced stomatal opening remain elusive. Genetic studies have revealed that several *Arabidopsis* mutants (e.g., *ca1ca4*, *ht1*, *ost1*, *slac1*, and *rboh*) showed different levels of insensitivity to low CO_2 induced stomatal opening and *ht1* completely lost the low CO_2 response (Hashimoto et al., 2006; Matrosova et al., 2015). The double mutant *ost1ht1* has an intermediate level of stomatal conductance of *ost1* and *ht1* mutants, but does not have a low CO_2 response, indicating HT1 is epistatic of OST1 in low CO_2 induced stomatal opening (Matrosova et al., 2015).

Except for the physiological and genetics studies, little is known about the molecular mechanisms including metabolic regulations underlying the guard cell low CO_2 responses. Small molecule metabolites are important regulators in stomatal movement with roles in osmotic regulation, signaling and redox regulation (Misra et al., 2015). For example, sugars, sugar alcohols and organic acids can contribute to the turgor pressure together with inorganic ions in course of stomatal movement. The most extensively studied organic osmolytes in guard cells are malate and sucrose (Lee et al., 2008; Lawson et al., 2014; Daloso et al., 2015a,b; Medeiros et al., 2016). Signaling molecules in guard cells include phytohormones (Daszkowska-Golec and Szarejko, 2013; Misra et al., 2015; Murata et al., 2015), lipids (Sakaki et al., 1995; Jung et al., 2002), zeaxanthin (Zeiger and Zhu, 1998; Zhu et al., 1998; Assmann, 1999), as well as cGMP (Pharmawati et al., 1998). The glutathione-ascorbate cycle is a well-known ROS scavenging pathway. In addition, flavonols have recently been shown to play a role in ROS scavenging, and can repress ABA induced stomatal closure (Watkins et al., 2014).

To discover new molecular components in low CO_2-induced stomatal opening, we applied hyphenated mass spectrometry (MS)-based metabolomics and proteomics approaches to analyze short-term low CO_2 responses in *B. napus* guard cells. The isolated guard cells were exposed to 400 ppm CO_2 (control) and 0 ppm CO_2 (treatment) and analyzed at five time points (0, 5, 10, 30, and 60 min). A total of 411 metabolites were quantified. We observed decreased trends of primary metabolites (e.g., most common amino acids, nucleotides and sugars), and changes in the levels of osmoregulators (e.g., increased levels of malate and mannitol at early and late time points). In contrast to guard cell elevated CO_2 response (Geng et al., 2016), JA biosynthesis was not altered in the low CO_2 response. Instead, phytohormones that induce stomatal opening, including cytokinins, auxins, gibberellins (GA), as well as melatonin increased at early time points. This study highlights the utility of single cell-type omics in discovering and testing new molecular components in cellular signaling and metabolic networks.

EXPERIMENTAL PROCEDURES

Plant Materials

B. napus var. Global seeds obtained from Svalöv Weibull AB (Svalöv, Sweden) were grown as previously described (Zhu et al., 2010). Fully expanded leaves from well-watered 7 weeks old plants were used for stomatal movement analysis and guard cell purification. *A. thaliana* mutant seeds *coi1-12* were provided by Dr. Zhonglin Mou, Department of Microbiology and Cell Science, University of Florida, and *ca1ca4* and *lox2* mutant seeds were obtained from the Arabidopsis Biological Resource Center (ABRC, Ohio State University, Columbus, USA). Seeds were germinated on a half strength Murashige and Skoog (MS) (Murashige and Skoog, 1962) medium prior to transferring to a Metro-Mix 500 potting mixture (The Scotts Co., Marysville, OH, USA). Arabidopsis plants were grown under a photosynthetic flux of 140 μmol photons m^{-2} s^{-1} and an 8 h light (22°C)/16 h dark (18°C) cycle for 6 weeks.

Preparation of Epidermal Peels for Stomatal Movement Assay

Small squares (0.5 × 0.5 cm^2) of leaf sections from 7 week-old *B. napus* plants were fixed abaxial side down onto coverslips coated with medical adhesive (Hollister, Libertyville, IL, USA). Adaxial epidermis and mesophyll layers were removed with a scalpel. After washing three times with distilled water to remove

cellular debris, the coverslips were incubated with a cell wall digesting enzyme mixture at 26°C, 140 excursions per min for 13 min on a reciprocal shaker. The digesting enzyme mixture was constituted as follows: 0.7% cellulase R-10 (Yakult Honsha Co., Ltd, Tokyo, Japan), 0.025% macerozyme R-10 (Yakult Honsha Co., Ltd, Tokyo, Japan), 0.1% (w/v) polyvinylpyrrolidone-40 (Calbiochem, Billerica, Massachusetts, USA), and 0.25% (w/v) bovine serum albumin (Research Products International Corp., Mt Prospect, Illinois, USA) in 55% basic solution (0.55 M sorbitol, 0.5 mM $CaCl_2$, 0.5 mM $MgCl_2$, 0.5 mM ascorbic acid, 10 μM KH_2PO_4, 5 mM 4-morpholineethanesulfonic acid (MES), pH 5.5 adjusted with 1 M KOH). The coverslips were then incubated in an opening buffer (10 mM KCl, 50 μM $CaCl_2$, 10 mM MES-KOH, adjusted to pH 6.15 with 1 M KOH) under light (110 μmol m^{-2} s^{-1}) for an hour. For low CO_2 treatment, the stomata were first stabilized in 400 ppm CO_2 balanced opening buffer for 15 min and then exposed continuously to 0 ppm CO_2 balanced opening buffer for a period of 60 min as previously described (Hu et al., 2010; Geng et al., 2016).

Large Scale Enriched Stomata Preparation for Proteomics and Metabolomics Analysis

Stomata from *B. napus* were prepared as previously described (Zhu et al., 2012; Geng et al., 2016). Briefly, the main and secondary veins of leaves were removed with a scalpel. Then the leaves were blended for 20 s each time for a total of four times in a blender (Sunbeam Products, Inc., Boca Raton, FL, USA) to remove the mesophyll cells. Epidermal peels were collected on a 100 μm nylon mesh and washed thoroughly with tap water to remove any broken cells. The peels were transferred to the enzyme mixture and digested as described above. Enriched stomata on digested peels were collected on the 100 μm nylon mesh and washed thoroughly with the opening buffer three times, and then transferred to the opening buffer in square petri dishes for recovery under light (140 μmol photons m^{-2} s^{-1}) at 22°C for an hour. All the samples were stabilized in 400 ppm CO_2 (control) for 15 min before continuing in control or switching to 0 ppm CO_2 treatment (Hu et al., 2010). The samples were collected at 0, 5, 10, 30, and 60 min on nylon meshes of 100 μm pore size, blotted dry quickly on filter paper, and transferred to Eppendorf tubes, and then quickly frozen (∼30 s) in liquid nitrogen and stored at −80°C before protein extraction. The samples for metabolomics were lyophilized to dryness before metabolite extraction.

Metabolite Extraction and Sample Preparation for Metabolomics

Each independent stomatal preparation was regarded as a replicate. A total of four replicates, each of 100 mg lyophilized sample were sent to Metabolon® Inc. (Durham, NC, USA) for GC-MS and UPLC-MS based metabolomic analyses. The samples were extracted sequentially with four different extraction solvents, i.e., 400 μL tridecanoic acid (2.5 mg/mL) dissolved in ethyl acetate:ethyl alcohol (1:1), 200 μL methanol, 200 μL methanol:H_2O (3:1), and 200 μL dichloromethane:methanol (1:1). Each extraction was carried out at 4°C on a Geno/Grinder 2000 homogenizer (with a 4 mm stainless steel ball added to each tube) (Glen Mills Inc., NJ, USA) for 2 min in the above specified extraction buffers, and the supernatants of each extraction were collected after centrifugation and pooled. Pooled extracts were divided into four equal aliquots, one used for GC-MS and three used for UPLC-MS. For GC-MS, the aliquots were lyophilized (Centrivac, Labconco Inc.) and further derivatized using 1:1 mixture of bistrimethylsilyl-trifluoroacetamide (Sigma, St. Louis, USA) and acetonitrile:dichloromethane:cyclohexane (5:4:1 by volume) with 5% trimethylamine and a series of alkylbenzenes used as retention index (RI) markers (Roessner-Tunali et al., 2003) at 60°C for 1 h. For UPLC-MS, the samples were also lyophilized and reconstituted in different loading solvents (water with 0.1% formic acid for reverse phase positive mode, 0.1% formic acid in 6.5 mM ammonium bicarbonate for reverse phase negative mode, and 10 mM ammonium formate for HILIC negative mode). The RI standards for the reverse phase positive mode include d7-glucose (RI 702), fluorophenylglycine (RI 1185), d3-methionine (RI 1237), d4-tyrosine (RI 1506), d3-leucine (RI 1666), d8-phenylalanine (RI 2027), d5-tryptophan (RI 2422), d5-hippuric acid (RI 2772), Br-phenylalanine (RI 3168), d5-indole acetate (RI 3740), d9-progeterone (RI 5298) and d4-diocylphthalate (RI 6118). Those for the negative mode include d7-glucose (RI 706), d3-methionine (RI 1134), d3-leucine (RI 1467), d8-phenylalanine (RI 1992), d5-tryptophan (RI 2264), Br-phenylalanine (RI 3058), Cl-phenylalanine (RI 3308), d15-octanoic acid (RI 4317), d19-decanoic acid (RI 5073), d27-tetradecanoic acid (RI 5423) and d35-octadecanoic acid (RI 5833).

Another set of four replicates of lyophilized samples (prepared separately) was used for our in-house targeted multiple reaction monitoring (MRM) HPLC-MS analyses (**Supplementary Table S1**) as previously described (Geng et al., 2016). Briefly, 10 μL internal standard mixture (100 μM lidocaine and 100 μM 10-camphorsulfonic acid for evaluating extraction efficiency) was added to each sample, and the samples were homogenized (with a 4 mm stainless steel ball in each tube) in liquid nitrogen for 20 s at 1900 strokes/min in a GenoGrinder (Geno/Grinder 2000, SPEX SamplePrep., Metuchen, NJ, USA). Metabolites were sequentially extracted in 1 mL of each extraction solvent, i.e., 80% methanol, acetonitrile:isopropanol:water (3:3:2), and acetonitrile:water (1:1) on a thermomixer (Thermomixer R, Eppendorf, Hamburg, Germany) at 4°C, 1,100 rpm for 15 min. Samples were then sonicated in ice water using a Branson® Ultrasonic Bath at 50 Hz for 15 min and centrifuged at 13,000 g for 15 min at 4°C. The combined supernatants were lyophilized at 160 mBar (Centrivap, Labconco Inc., USA) and re-dissolved in 100 μL water at room temperature for 15 min. After centrifugation at 4°C, 13,000 g for 15 min, the supernatants were used for MRM HPLC-MS.

GC-MS, UPLC-MS and MRM HPLC-MS Analyses

Samples for GC-MS and UPLC-MS analyses were profiled as previously described (Lawton et al., 2008; Evans et al., 2014). Briefly, derivatized GC-MS samples were separated on a 5%

diphenyl/95% dimethyl polysiloxane fused silica column (20 m × 0.18 mm ID; 0.18 um film thickness, Thermo Scientific Inc.) with helium as carrier gas and a temperature ramp from 60 to 340°C in 17.5 min, followed by detection on a Trace DSQ quadruple mass spectrometer with electron impact ionization (Thermo Scientific Inc., San Jose, CA, USA). For UPLC-MS, the columns were a Waters UPLC BEH C18 (2.1 × 100 mm, 1.7 μm) column for reverse phase chromatography, and a Waters UPLC BEH Amide (2.1 × 150 mm, 1.7 μm) column for the hydrophilic interaction liquid chromatography (HILIC) separation. The solvents used for reverse phase positive mode were 0.1% formic acid in water (solvent A) and methanol (solvent B), for reverse phase negative mode is 6.5 mM ammonium bicarbonate in water (A) and methanol (B), and for HILIC negative mode is 10 mM ammonium formate in water (A) and acetonitrile (B). The gradient of solvent B for reverse phase was ramped from 0.5 to 70% in 4 min, then from 70 to 98% in 0.5 min, held at 98% for 0.9 min, then return to 0.5% in 0.2 min, and finally held at 0.5% for 5.4 min. The flow rate was 0.35 mL/min. The gradient for HILIC was ramped from 5 to 50% in 3.5 min, then to 95% in 2 min, held at 95% for 1 min, and back to 5% in 0.2 min and held at 5% for 4.3 min. The flow rate was 0.5 mL/min. The Waters ACQUITY UPLC was connected to a Thermo Scientific Q-Exactive mass spectrometer interfaced with a heated electrospray ionization (HESI-II) source. The MS analysis alternated between MS and data-dependent MS2 scans using dynamic exclusion, and the scan range was from 80 to 1,000 m/z. The spray voltage for reverse phase positive mode, negative mode and HILIC negative mode was 4, 2.75, and 3 kV, respectively. The sheath gas and auxiliary gas settings for reverse phase positive mode were 40 arbitrary units (au) and 5 au, respectively. Those for reverse phase negative mode were 75 au and 15 au, respectively, and for HILIC were 40 au and 5 au, respectively. The source heater temperature for reverse phase positive and negative mode was 400°C, and for HILIC was 380°C. The normalized collision energy setting for reverse phase positive mode, negative mode and HILIC negative mode was 40, 60, and 60%, respectively.

HPLC-MRM-MS was conducted using an Agilent 1100 HPLC (Agilent, Santa Clara, CA, USA) coupled with an AB Sciex 4000 QTRAP™ (AB Sciex, Framingham, MA, USA). An Agilent, Eclipse XDB-C18 column (4.6 × 250 mm, 5 μm) was used for metabolite separation with 0.1% formic acid in water as solvent A and 0.1% formic acid in acetonitrile as solvent B. The HPLC gradient started at 1% solvent B for 5 min, then a linear gradient from 1 B to 99.5% B over 41.5 min, held at 99.5% B for 4.5 min, and then return to 1% B in 0.3 min and held at 1% B for 8.7 min. The flow rate was 0.5 mL/min. The mass spectrometer conditions were: 30 psi curtain gas, 50 psi GS1, 55 psi GS2, ion source voltage 4,500 V, with a TurboIon electrospray ionization (ESI) interface temperature of 350°C. A multiple period method was used as previously described (Chen et al., 2013; Geng et al., 2016). Briefly, MRM-transitions were separated into different periods based on the compounds retention time to increase the number of compounds that can be detected in a single run. The five periods in positive mode were separated at 5.8, 15.7, 23.7, 36.2, and 60 min. The three periods in negative mode were separated at 15.9, 26.32, and 60 min. Both positive and negative modes use the same HPLC gradient as described above. Detailed compounds in each period of the MRM method can be found in **Supplementary Table S1**.

Metabolomics Data Processing, Statistics and Pathway Analysis

All data were combined to a final peak list (**Supplementary Table S1**). The data processing method was described in detail in previous publications (Evans et al., 2009, 2014). Briefly, a Metabolon in-house software was used for metabolite peak detection and integration. Extracted ion chromatograms were binned by mass. After determining the baseline noise, MS peaks were determined and peak areas were calculated based on these criteria: smoothing of 7–9, signal to noise >5, height threshold of 20,000, width threshold of 0.035, area threshold of 20,000, and 10% zero scans (essentially permitted number of missing scans allowed for peak to be considered real). Individual MS peaks were grouped by apex retention time, and the chromatograms were aligned based on RI values. The RI of a compound is a number, obtained by logarithmic interpolation, relating the adjusted retention volume (time) or the retention factor of the compound to the adjusted retention volumes (times) of two RI standards (whose RI values were set) eluted before and after the peak of the sample component (Kováts, 1958; Evans et al., 2009). The output data after peak detection and integration contained m/z ratios, RIs and peak areas.

Metabolite identification was relied on comparing RI, accurate mass +/− 0.005 amu and MS/MS spectral data with the authentic compound information in the Metabolon library. The RI should be within 75 RI units of the proposed identification (Evans et al., 2009). The MS/MS matching is based on a comparison of the ions present in the experimental spectrum to the ions present in the library spectrum. All proposed identifications were manually reviewed and hand curated based on the above mentioned criteria. For metabolites identified from multiple platforms (e.g., GC-MS and LC-MS), only one call of highest quality for a given compound (with symmetry narrow peak and a tailing factor close to 1, as well as lack of interference from adjacent compounds based on isotopic patterns) was chosen so that the statistics will not be skewed. If one platform had missing data (nulls) and another had values for the samples, the latter was chosen. The peak area (raw) for one ion in each compound spectrum was used for quantification. The data have no units, and represent relative quantification. Comparisons of peak values are valid only within each compound individually, across all samples. Missing values were imputed using a k-Nearest Neighbor (KNN) method (Hastie et al., 2014). Differentially changed metabolites were analyzed using R-based empirical analysis of digital gene expression (EDGE) package in R (version 3.2.5) (R Development Core Team, 2015) as previously described (Jin et al., 2013; Storey et al., 2015). Comparisons were made between treatment and control samples for each time point. The full model used CO_2 concentration as the variable of interest, replicate batch as adjustment variables, and a null model used only replicate batch as adjustment variables. The R package uses likelihood ratio test

to generate *p*-values. A total of 2,000 bootstrap iterations were performed for each comparison. Metabolic pathway analyses were performed for metabolite comparisons at each time point using MetaboAnalyst 3.0 (Xia et al., 2015). Raw data were uploaded to MetaboAnalyst 3.0 webserver and only metabolites mapped to the KEGG pathway database were used. A $\log_2$ transformation was used to normalized and scale the data before further analysis.

Protein Extraction and Tandem Mass Tag (TMT) 10-Plex Labeling

Enriched stomata samples (each of 100 mg fresh weight) were ground with a mortar and a pestle in liquid nitrogen into fine powder, which was transferred to a 40 mL Oakridge tube. Then 1.25 mL of 10 mM Tris-HCl, pH 8.0 saturated phenol and 1.25 mL of extraction buffer (0.1 M Tris-HCl pH8.8, 10 mM EDTA, 0.4% β-mercaptoethanol and 0.9 M sucrose) were added to the sample sequentially. The mixture was agitated at room temperature for 2 h, followed by centrifugation at 4°C, 5,000 g for 10 min. The phenol layer was transferred to a new tube, and another 1.25 mL phenol was added to the bottom layer to back extract at room temperature for 30 min. The phenol layer was combined with the previous extraction and protein was precipitated with 5 volumes of cold 0.1 M ammonium acetate in 100% methanol at −20°C overnight. The protein was then pelleted by centrifugation at 4°C, 20,000 g for 20 min. The pellet was washed twice with 0.1 M ammonium acetate, twice with 80% acetone and once with 100% acetone. Protein amounts were assayed using a EZQ assay kit (Thermo Scientific Inc.) according to manufacture instructions. A total of 30 μg protein each sample was dissolved in 50 μl 100 mM triethyl ammonium bicarbonate (TEAB) buffer, followed by reduction with 17 mM Tris (2-carboxyethyl) phosphine at room temperature for 30 min and alkylation with 10 mM iodoacetamide for 1 h in the dark. Six volumes of pre-chilled (−20°C) acetone was used to precipitate the protein at −20°C overnight. Samples were then centrifuged at 4°C at 8,000 g for 10 min. Supernatant was carefully removed and pellets were left to dry for 2–3 min. Then, 50 μL of 100 mM TEAB was used to re-dissolve the sample and 1.5 μg of trypsin was used to digest the protein at 37°C overnight. TMT labels 126, 127N, 127C, 128N, 128C, 129N, 129C, 130N, 130C, and 131 were used to label samples collected at 0 min, 5 min control, 5 min treatment, 10 min control, 10 min treatment, 30 min control, 30 min treatment, 60 min control, 60 min treatment, and a universal control sample, respectively. Samples were labeled for 1 h and then quenched with 4 μL of 5% hydroxylamine for 15 min. All samples were then combined, lyophilized, and reconstituted in 100 μL 0.1% TFA (trifluoroacetic acid) solution. A Macrospin C-18 reverse phase mini-column with a capacity of 30–300 μg (The Nestgroup Inc., Southborough, MA, USA) was used to desalt the samples. Two independent replicate TMT experiments were conducted.

Strong Cation Exchange Fractionation and UPLC-MS/MS Analysis of Peptides

The TMT labeled peptides were fractionated using an Agilent HPLC 1260 on a polysulfoethyl A strong cation exchange (SCX) column (2.1 × 100 mm, 5 μm, 300 Å, PolyLC, Columbia, USA). Solvent A was 25% (v/v) acetonitrile, 10mM ammonium formate and 0.1% (v/v) formic acid (pH 2.8), and solvent B was 25% (v/v) acetonitrile and 500 mM ammonium formate (pH 6.8). The gradient for solvent B was at 0% for 10 min, then ramped up to 20% in 80 min and to 100% in 5 min, held at 100% for 10 min. Peptide elution was monitored at 280 nm and 12 fractions were collected for UPLC-MS/MS.

The SCX fractions were analyzed on an Easy-nLC 1200 system coupled to a Q-Exactive Orbitrap Plus MS (Thermo Fisher Scientific, Bremen, Germany). The peptides were concentrated on an Acclaim PepMap 100 pre-column (20 mm × 75 μm; 3 μm-C_{18}), then separated on a PepMap RSLC analytical column (250 mm × 75 μm; 2 μm-C_{18}). Water and 80% acetonitrile with 0.1% formic acid were used as solvent A and B, respectively. The gradient for solvent B ramped from 2 to 30% in 100 min, from 30 to 98% in 10 min, then held at 98% for 10 min. The flow rate was 350 nL/min. Positive ion mode with data dependent scanning and higher-energy collision dissociation (HCD) was used as previously described (Jones et al., 2013). The full MS resolution was 70,000 with a scan range of 400–2,000 m/z, an automatic gain control (AGC) target of $1e^6$ and maximum ion trapping (IT) of 100 ms. The tandem mass spectrum resolution was 35,000, an AGC target of $2e^5$, maximum injection time of 117 ms, a loop count of 10, an isolation window of 1.3 m/z, a fixed first mass of 115 m/z and a normalized collision energy setting of 32%. A lock mass of polysiloxane ion (445.12,003 m/z) was used for real-time mass calibration. The spray voltage was set to be 1900 volts, capillary temperature was 320°C, and the stacked ring ion guide radio frequency voltage was set to 70 V.

Protein Identification and Quantification

Peptides were identified using Proteome Discoverer 1.4 software (Thermo Fisher Scientific, Bremen, Germany), searched against a modified *B. napus* database downloaded from Genescope (Chalhoub et al., 2014). Redundant sequences were first removed with patpd program from AB-BLAST 3.0 (Gish, 1996-2009), then subjected to redundant entry clustering using the perl script nrdb90 with an identity level at 95% (Holm and Sander, 1998). The final database contains 79,366 non-redundant proteins. The annotation was done by blasting against the non-redundant green plant database from NCBI using Blast2Go (Conesa and Götz, 2008). The searching parameters include 20 ppm tolerance for precursor mass tolerance, and 0.02 Dalton for fragment mass tolerance, two missed cleavages, TMT10-plex label on the N-terminal, carbamidomethylation (C), oxidation (M), phosphorylation (S, T, Y), and deamidation on the N-termini. Peptides were filtered using stringent Xcorr value cut off at 2.31 for 2+, 2.41 for 3+, 2.6 for 4+ and 5+ peptides. Peptide quantification result was exported for further processing and statistical analysis. The peptide quantification was first normalized by the mean of each tag, then sum of the same peptide was calculated. Only peptides that were present in the two independent experiments and unique for their corresponding proteins were used for protein quantification. All the identified peptides and proteins are listed in **Supplementary Table S2**. Ratios of 0 ppm CO_2 treated samples to 400 ppm CO_2 treated controls were calculated for each time point (127C/127N for 5 min, 128C/128N for 10

min, 129C/129N for 30 min, 130C/120N for 60 min). Fold changes for proteins were the means of all unique peptides identified from the corresponding proteins. Student's *t*-tests were performed with the $\log_2$ transformed fold changes for each time point. A singular enrichment analysis (SEA) was performed for proteins with a *p*-value less than 0.05 using agriGO (Du et al., 2010).

RESULTS

Low CO_2 Induced Stomatal Opening and Metabolomic Changes

To determine the time points for metabolite measurement, *B. napus* stomatal movements in response to ambient (400 ppm) and low (0 ppm) CO_2 conditions were recorded at different time points. Stomatal aperture under low CO_2 treatment gradually increased, and became significantly different from the ambient control samples at 5 min and onwards (**Figure 1**). The fast response to low CO_2 took place within 20 min. At 60 min, there was only a slight increase in stomatal aperture relative to the previous three time-points (**Figure 1**). Based on this data, we chose to collect our guard cell samples at 0, 5, 10, 30, and 60 min after the low CO_2 treatment.

Using hyphenated-MS based metabolomics platforms, we identified 411 non-redundant metabolites in stomatal guard cells. The numbers of differentially changed metabolites at each time point were shown in **Figure 2A**. Before 30 min of low CO_2 treatment, there were more increased metabolites than decreased ones. At 60 min, the decreased metabolites outnumbered the increased metabolites (**Figure 2A**). The initial increase in many metabolites could be attributed to catabolism from large storage molecules and production of osmolytes needed for turgor and stomatal opening. At 60 min, more decreased metabolites may reflect decreased inorganic carbon source under the low CO_2 condition. The significantly accumulated metabolites are specific to each time point and belong to different metabolic pathways. At 5 min, pathway enrichment analysis revealed that intermediates in unsaturated fatty acid biosynthesis were significantly over-represented among the significantly altered metabolite levels. At 5 min and 10 min, fatty acid and flavonoid biosynthesis were over-represented (**Figures 3**, **4**), and these two pathways were also found to be responsive to elevated CO_2 (Geng et al., 2016).

Lipid Metabolism in Guard Cells under Low CO_2

Lipid metabolism showed significant changes at 5 min and 10 min based on the pathway enrichment result (**Figure 3**).

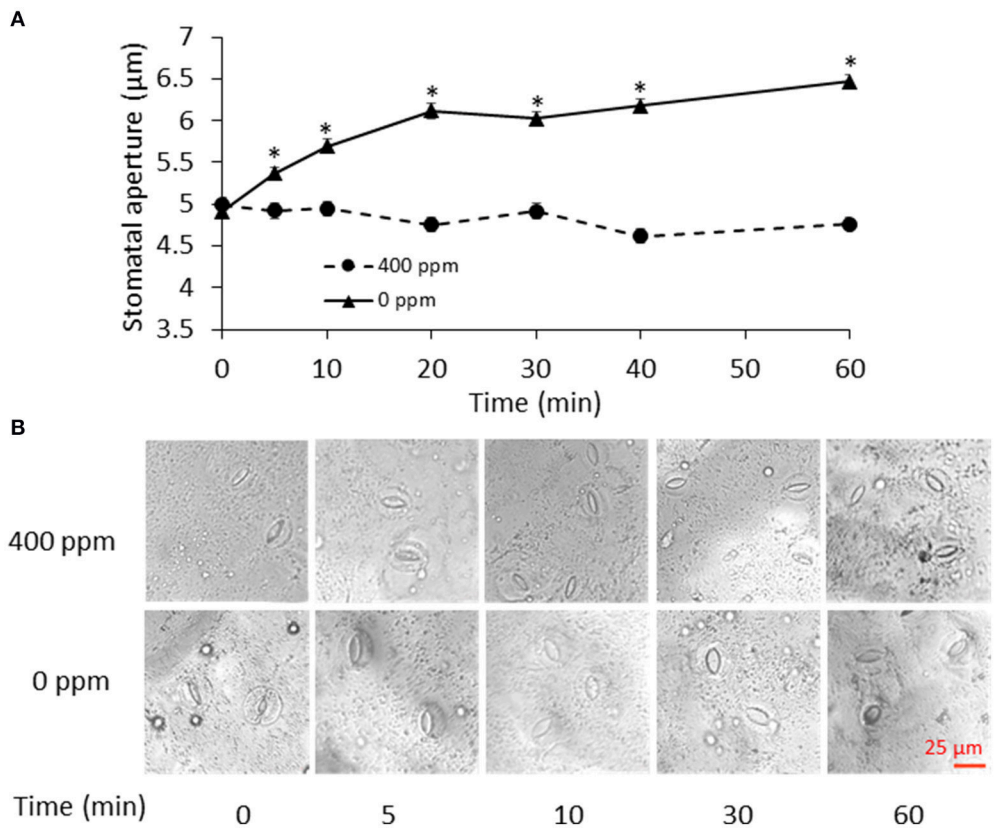

FIGURE 1 | Stomatal movement in response to low CO_2. **(A)** Time course of stomatal movement under atmospheric (400 ppm) and low CO_2 (0 ppm) conditions. Data are mean ± standard error of three independent experiments ($n = 3$) with 60 stomata counted for each replicate. *$p < 0.05$, Student's *t*-test. **(B)** Representative images of stomatal aperture during the control atmospheric CO_2 and low CO_2 treatments. Scale bar indicates 25 μm.

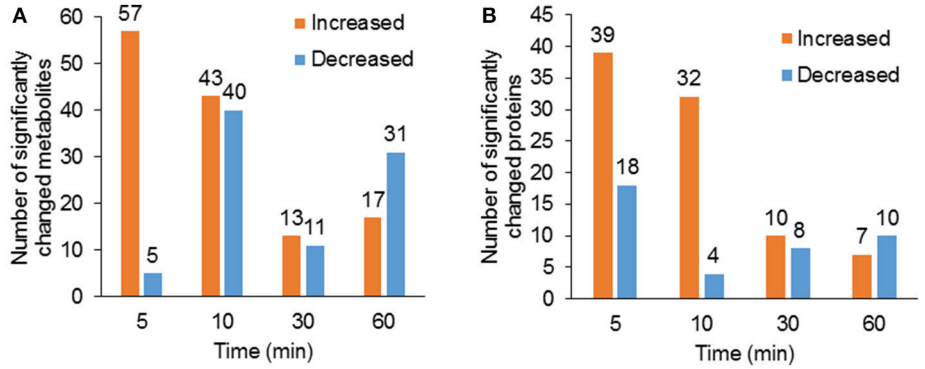

FIGURE 2 | Overview of significantly changed metabolites and proteins under low CO_2 condition. **(A)** Total number of significantly increased ($p < 0.05$, fold change >1.2) and decreased ($p < 0.05$, fold change <0.8) metabolites at each time point of the treatment. **(B)** Total number of significantly increased and decreased proteins at each time point of the treatment.

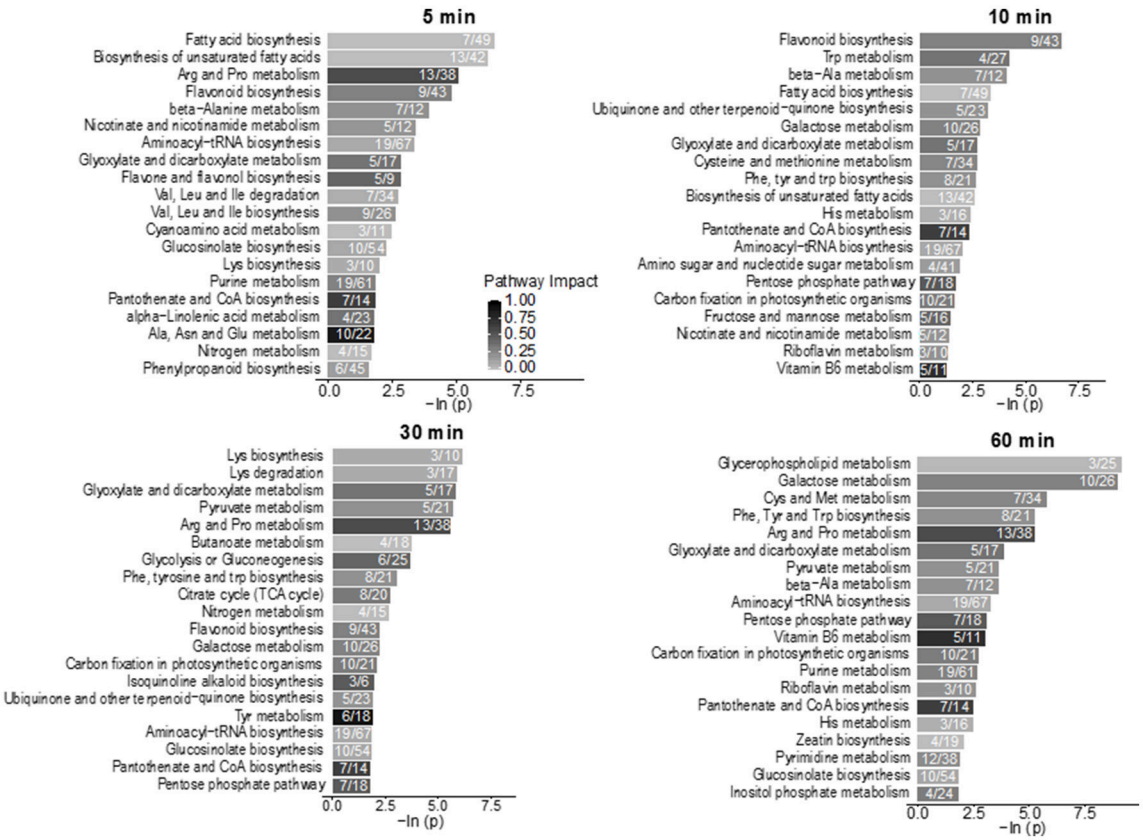

FIGURE 3 | Pathway enrichment analysis of the low CO_2 responsive metabolites in the time-course study. Numbers inside the bars indicate the number of metabolites that matched to the total metabolites in that pathway. Only pathways with four or more metabolites that matched were included in the analysis. The scale bar of different levels of grayness indicates pathway impact.

Since many of the lipids identified cannot be assigned with a Kyoto Encyclopedia of Genes and Genomes (KEGG) ID, here we manually examined the lipid species detected, which were mainly short chain free fatty acids and monoacylglycerol (**Supplementary Table S1**). At 5 min, most lipids and fatty acids increased, but after 10 min most lipids decreased (**Figure 4**). This trend of change was similar for both saturated and unsaturated lipids, irrespective of their different chain lengths. Free fatty acid accumulation during the low CO_2 induced stomatal opening could be caused by increased hydrolysis of

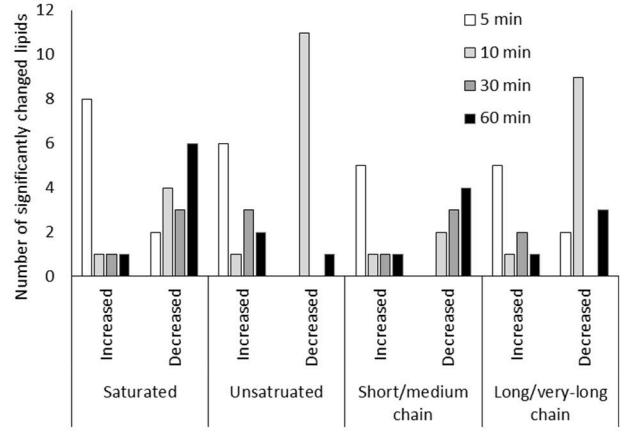

FIGURE 4 | Lipid metabolic changes in guard cells under low CO_2. Short/medium chain lipids include lipids of 5C-14C lipids. Long/very-long chain lipids include lipids with carbon chains longer than 16C. Only lipids that showed significant changes ($p < 0.05$) were included.

intracellular lipids, increased de-novo synthesis or decreased consumption by free fatty acid-consuming pathways. The mechanisms causing subsequent decreases in free fatty acids after 10 min are unknown, but could be explained by their incorporation into membranes or catabolism for energy production. Interestingly, our proteomics data showed that under low CO_2, proteins involved in catabolism process are enriched (**Supplementary Figure S1**). Thus, the initial increase in fatty acids is likely due to the breakdown of storage lipids. Concomitantly, at 5 min two GDSL (Glutamate-Aspartate-Serine-Leucine) motif containing esterases/lipases were found to be significantly increased (**Supplementary Table S3**) and these enzymes usually exhibit broad substrate specificity and multi-functionality (Chepyshko et al., 2012). Whether they directly hydrolyze storage lipids is not known.

At 5 min, two phospholipids (**Supplementary Table S1**) and a phospholipase Dα (**Supplementary Table S3**) decreased. The product of phospholipase Dα has been shown to be a positive regulator of ABA induced stomatal closure (Zhang et al., 2009). Thus, the decreased levels of phospholipids and phospholipase are consistent with the stomatal opening phenotype under low CO_2 (**Figure 1**).

Phytohormone Changes in Guard Cells under Low CO_2

Jasmonic acids were previously shown to be involved in high CO_2 induced stomatal closure (Geng et al., 2016). Under low CO_2, however, we only observed an increase of the intermediate 13S-hydroperoxy-9Z,11E,15Z-octadecatrienoic acid (13-HPOT), which is a precursor for jasmonates (JAs) and traumatic acid production. No significant changes were found in jasmonic acid, methyljasmonic acid or 12-oxo-phytodienoic acid. Interestingly, traumatic acid showed more than 7-fold increases after 10 min of low CO_2 treatment (**Figure 5**). That traumatic acid and not jasmonic acid was accumulated indicates that traumatin may be more important than JAs in low CO_2 induced stomatal opening. We then tested the stomatal movement of JA biosynthesis mutant *lox2* and signaling mutant *coi1*. Both mutants were still able to open stomata in response to low CO_2 (**Figure 5**), confirming that JAs are not involved in guard cell low CO_2 response. Similar to JAs, abscisic acid (ABA) did not show significant changes under low CO_2, but ABA catabolic products, phaseic acid (1.49-fold at 5 min) and dihydrophaseic acid (>2.4-folds after 10 min) showed significant increases (**Supplementary Table S1**). As expected, hormones known to induce stomatal opening, e.g., auxins, cytokinins, brassinosteroids, gibberellins all showed increasing trends under low CO_2 (**Figure 6**). In addition, melatonin, a well-studied animal hormone regulating circadian rhythms and various biological processes and discovered in plants in 1995 (Arnao and Hernandez-Ruiz, 2006; Nawaz et al., 2016, was found to increase at 5 min and 10 min of low CO_2 treatment (**Figure 6**). Except for zeatin riboside, all other hormones increased at early time points at 5 or 10 min. These data suggest that low CO_2 induced stomatal opening is a multi-hormone response.

Protein Changes in Guard Cells under Low CO_2

To complement the metabolomics data, we performed a proteomic analysis of the samples used for metabolomics. The number of significantly changed proteins showed similar trends of changes as metabolites (**Figure 2B**). Single enrichment analysis was performed for proteins that show significant changes at one or more time points. The differentially accumulated proteins were enriched in metabolic processes, especially oxidation/reduction, catabolism/ proteolysis, and cellular nitrogen metabolism processes. In terms of molecular functions, these proteins were enriched in catalytic activity, protein and nucleotide binding, and antioxidant activity (**Supplementary Figure S1**). Here we discuss some examples (please refer to **Supplementary Table S3** for detailed results of significant protein changes).

At 5 min a V-type ATPase subunit G1 was significantly increased (1.3-fold change, with a *p*-value of 0.03), and so was another subunit A2 at 10 min (1.4-fold, with a *p*-value of 0.04). The increase of V-type ATPases may cause cytosolic acidification under low CO_2 and promote stomatal opening. Guard cell V-type ATPase activity was found to be insensitive to ABA or fusicoccin (Willmer et al., 1995), so it is possible that the V-type ATPase represents specific low CO_2 response. At 5 min, a probable aquaporin PIP2-5 was increased (1.4-fold, with a *p*-value of 0.04). Aquaporin is one of the passages for CO_2 intake. Although a knockout mutant *pip2;1* did not show any significant changes compared to wildtype in the course of high CO_2 induced stomatal closure, PIP2-1 has been implicated in CO_2 signal transduction since it physically interacts with CA4 located on the plasma membrane (Wang et al., 2016). How PIP2-5 functions in guard cell low CO_2 response is intriguing. At 10 min, a voltage dependent potassium channel increased by 1.2-fold. The increases of the above mentioned membrane transport-related proteins may play important roles in promoting stomatal opening under

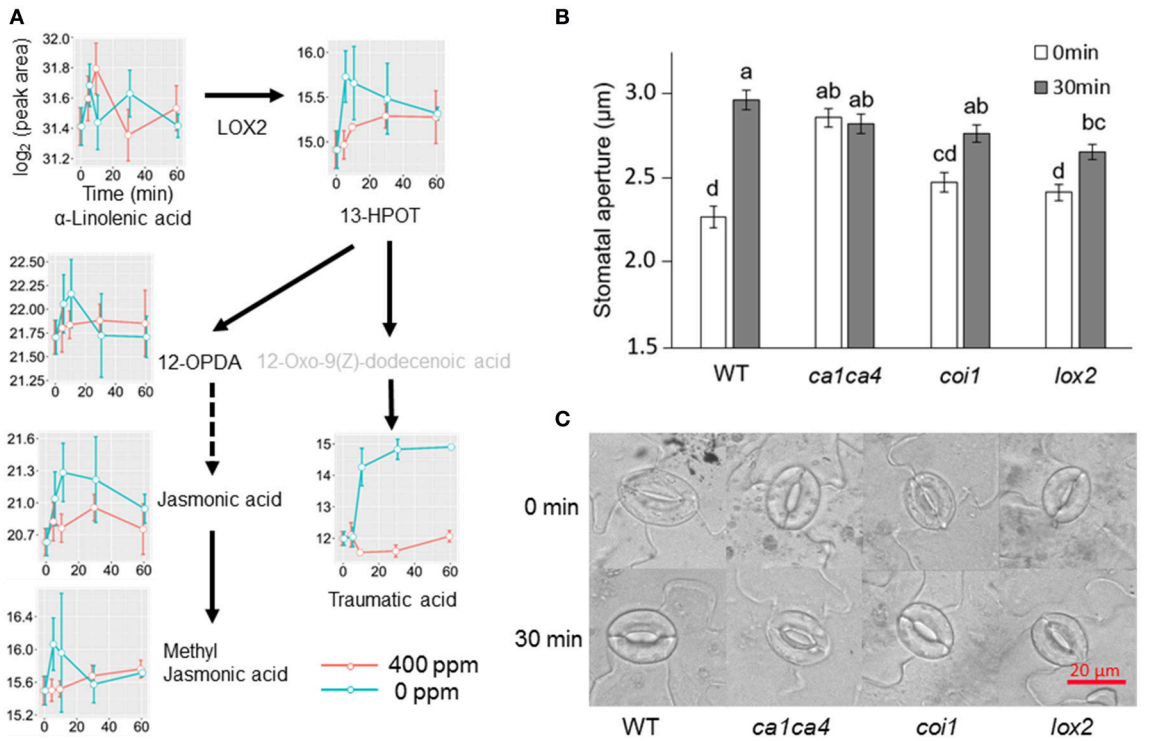

FIGURE 5 | Metabolite changes in JA and traumatic acid pathways and stomatal low CO_2 response of *A. thaliana* mutants. **(A)** Changes of metabolites in JA and traumatic acid pathways in *B. napus* guard cells under low CO_2 treatment. 13-HPOT, (9Z,11E,15Z)-(13S)-13-Hydroperoxyoctadeca-9,11,15-trienoic acid; 12-OPDA, (15Z)-12-Oxophyto-10,15-dienoic acid; **(B)** Stomatal movement of JA biosynthesis and signaling mutants after low CO_2 treatment. Data are mean ± standard error of three independent experiments ($n = 3$) with 60 stomata counted for each replicate (i.e., a total of 180 stomata). Two-way ANOVA and Tukey's test were used for stomatal movement analysis between different time points and different genotypes; **(C)** Representative images of stomatal aperture of **(B)**.

low CO_2. In addition, a subtilisin-like protease 2 was found to be increased at 5 min (1.5-fold, with a p-value of 0.03). Subtilisin-like protease SSD1 was shown to cleave EPIDERMAL PATTERNING FACTOR 2 (EPF2), producing the active form of EPF2. Loss of SSD1 was reported to enhance the elevated CO_2 induced decrease of stomatal index (Engineer et al., 2014). It is reasonable to predict that increased SSD protein level may increase stomatal index under long-term low CO_2 treatment.

Consistent with the phytohormone changes described in the previous section, auxin transporter 3 and gibberellin-regulated 14 like protein were found to increase significantly at 5 min (1.4-fold, with a p-value of 0.03) and 10 min (1.3-fold, with a p-value of 0.04), respectively. Another interesting change is the significant decrease of an isoflavone reductase homolog P3-like at 30 min after low CO_2 treatment (0.76-fold, with a p-value of 0.01). Isoflavone reductase was reported to function as an antioxidant in response to ROS (Kim et al., 2010; Watkins et al., 2014). ROS burst is known to play an important signaling role in the regulation of stomatal closing processes (Watkins et al., 2014; Murata et al., 2015; Geng et al., 2016; Sierla et al., 2016), but it has not been observed in the stomatal opening process. The decrease of isoflavone reductase constitutes another line of evidence for the lack of ROS burst in the low CO_2 induced stomatal opening.

DISCUSSION

Fatty Acid and Energy Metabolism are Important in Stomatal Low CO_2 Response

In general, primary metabolism in guard cells under low CO_2 is skewed toward catabolism. Recently, it has been shown that breakdown of storage triacylglycerol is an essential step for light induced stomatal opening, and the free fatty acids generated may be utilized for energy production to promote stomatal opening (McLachlan et al., 2016). In this study, an initial increases of free fatty acids and monoglycerol lipids were observed under low CO_2 induced stomatal opening (**Figures 3**, **4**), and two GDSL esterase/lipases increased concomitantly (**Supplementary Table S3**). These data suggest that the breakdown of storage lipids in response to low CO_2 may function similarly as light induced stomatal opening. Additionally, membrane expansion is needed for the stomatal opening process, thus the generated free fatty acids may also be utilized for new membrane lipid synthesis. Furthermore, the increase of two Ras-related proteins (both 1.3-folds, with p-values of 0.04) at 5 min and 10 min of low CO_2 treatment indicates involvement of membrane signaling. Roh family members of the Ras-related G proteins (ROPs) were found to be involved in endocytosis processes during ABA and high

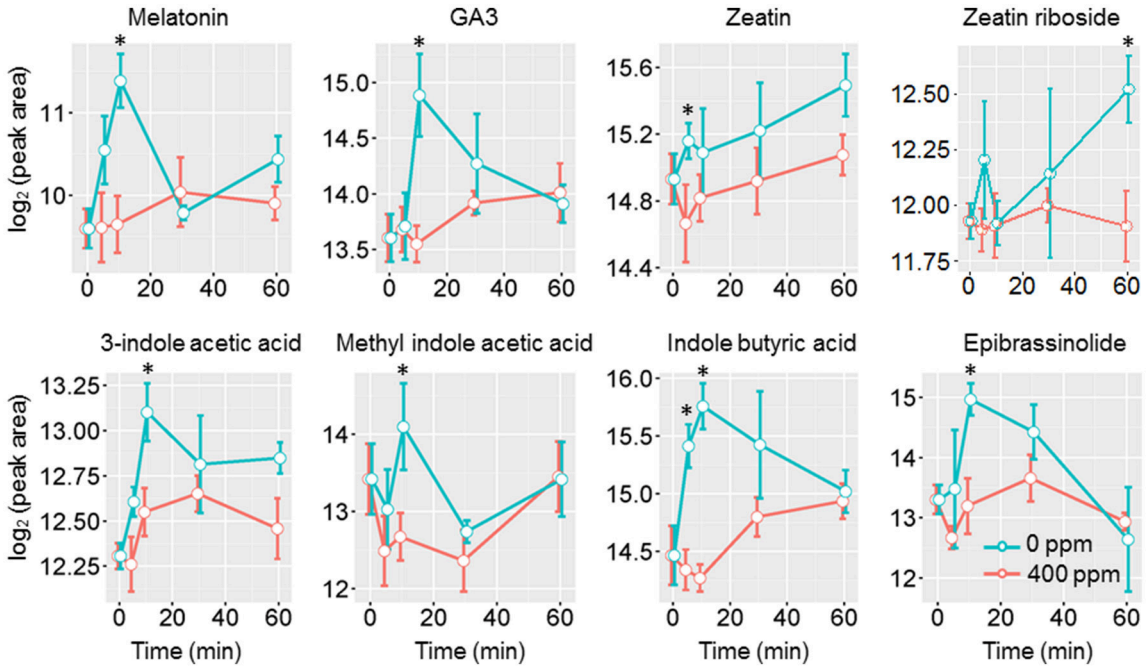

FIGURE 6 | Phytohormone level changes in guard cells under low CO_2. Student's *t*-test was performed between atmospheric control and low CO_2 treatment at each time point. Star (*) indicates $p < 0.05$.

CO_2 induced stomatal closure, and active ROP2 GTPase caused inhibition of ABA and elevated CO_2 induced stomatal closure (Hwang et al., 2011). Thus, the increase of Ras-related proteins could promote stomatal opening, and this hypothesis needs to be further tested.

Stomatal opening requires energy, which can come from photosynthesis or respiration. Although the importance of guard cell photosynthesis has been under debate (Santelia and Lawson, 2016), our metabolomics data suggests significant contribution of glycolysis, starch and sucrose metabolism, and pentose phosphate pathway to low CO_2 induced stomatal opening (**Figures 3**, **7**). GO term enrichment of significantly changed proteins indicates significant changes in glycolysis pathway (**Supplementary Figure S1**). Proteins involved in glycolysis and TCA cycle, including glycerol-3-phosphate dehydrogenase, fructose-bisphosphate aldolase, enolase/phosphopyruvate hydratase, aconitate hydratase, and pyruvate dehydrogenase E1 component subunit alpha, all increased at both early and later time points (**Supplementary Tables S2**, **S3**). A recent study using chlorophyll-less guard cells showed that guard cell CO_2 response does not depend on photosynthesis (Azoulay-Shemer et al., 2015), indicating respiration may be the main source of energy production during CO_2 induced stomatal movement.

Phytohormone Crosstalk Mediates Low CO_2 Induced Stomatal Opening

Under low CO_2, many phytohormones that induce stomatal opening may orchestrate to facilitate the opening process. Auxins were found to counteract ABA induced stomatal closure by preventing ROS and NO production (She and Song, 2006; Song et al., 2006). Cytokinins can scavenge the ROS and NO present in the cells, as well as prevent further ROS and NO production (She and Song, 2006; Song et al., 2006). Brassinosteroid (BR), on the other hand, can induce stomatal opening or closing depending on the concentration. A BR deficient mutant was shown to be hypersensitive to ABA induced stomatal closure (Ephritikhine et al., 1999), indicating BR also counteracts ABA. It has become clear that low concentrations of BR induce stomatal opening, while high concentrations can cause stomatal closure (Xu et al., 1994a,b; Haubrick et al., 2006). As expected, hormones known to induce stomatal opening, e.g., auxins, cytokinins, BR, gibberellins all showed increasing trends under low CO_2. In addition, melatonin was also found to increase at 5 min and 10 min of low CO_2 treatment (**Figure 6**).

Previously, we have found that JAs were involved in high CO_2 induced stomatal closure (Geng et al., 2016). Under low CO_2, we did not observe any significant changes of JAs (**Figure 5**). Instead, traumatic acid was found to be increased, implying its potential involvement in low CO_2 induced stomatal opening. Work on drought stress in rice confirmed the competition of traumatic acid production with JA production (Liu et al., 2012). Similar to JAs, ABA levels did not show significant changes despite the increases of ABA catabolic products phaseic acid and dihydrophaseic acid under low CO_2 treatment. These data suggest that low CO_2 induced stomatal opening is a multihormone response. How the recently discovered metabolites (e.g., melatonin and traumatic acid) function in the guard cell low CO_2 response and how they crosstalk with other hormones deserve further studies.

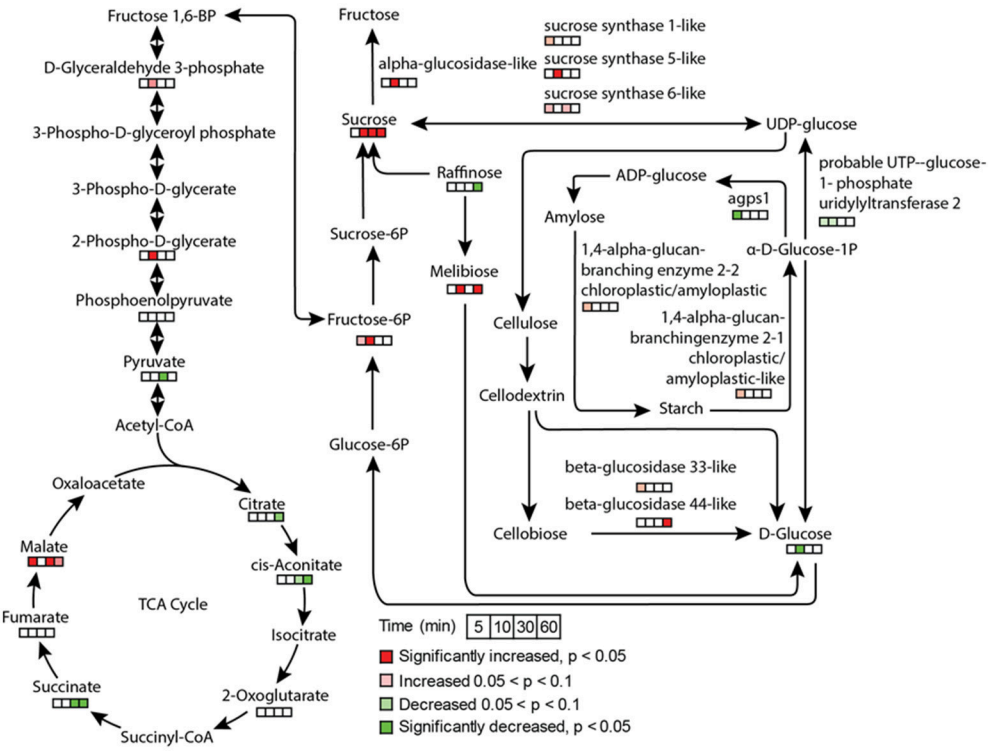

FIGURE 7 | Metabolite and protein changes in response to low CO_2 treatment in glycolysis, TCA cycle, and sucrose and starch metabolism. The pathways were drawn based on KEGG pathway database. The metabolites and proteins detected were indicated by time course square bars right below the molecules.

Comparison between High CO_2 and Low CO_2 Responsive Metabolites in Guard Cells

Here we compare the metabolite changes under low CO_2 (this study) and high CO_2 (Geng et al., 2016) to better understand CO_2 regulation of guard cell metabolism and signaling. Interestingly, the changes in many different groups of metabolites, especially phytohormones, flavonoids, sugars and sugar alcohols showed opposite trends under the two CO_2 treatment conditions (**Supplementary Figure S2**) (Geng et al., 2016). Phytohormones known to induce stomatal opening, including auxin, cytokinin and gibberellin all showed increases under low CO_2 but not under elevated CO_2. On the other hand, phytohormones that promote stomatal closure, such as ABA and JAs showed increases under elevated CO_2 (Geng et al., 2016), but no significant changes under low CO_2 (see previous section). In addition, we also found significant increases of melatonin at 5 min and 10 min of low CO_2 treatment, and significant decreases under elevated CO_2 (**Figure 6**, **Supplementary Figure S2**). Treatment with melatonin can inhibit plant ABA response by attenuating the ROS production, as well as repressing the expression of ABA biosynthesis genes and activating ABA catabolic genes (Li et al., 2015). How melatonin functions in guard cell CO_2 responses is a very interesting question for future studies.

Two groups of flavonols, quercetins, and kaempferols were transiently increased at 5 min and 10 min under elevated CO_2 (Geng et al., 2016). However, under low CO_2, both metabolites showed decreases (**Supplementary Table S1**). Since flavonols have been indicated to be ROS scavengers, the decreases of antioxidants correlate well with the notion of minimal ROS production in guard cells under low CO_2. Then how were ROS levels controlled under low CO_2 conditions? At the proteome level, we observed that the significantly changed proteins were enriched in cell redox homeostasis processes (**Supplementary Figure S1**). These proteins include four peroxidases, a superoxide dismutase, a peroxisomal ascorbate peroxidase, two NADH-ubiquinone oxidoreductases, a sulfate reductase, a sulfate oxidase, and others involved in various cellular redox regulation processes. Most of the proteins such as peroxidases showed significant increases (**Supplementary Table S3**), suggesting their function of maintaining low levels of ROS to promote stomatal opening under low CO_2. Consistent with this interpretation, metabolites related to ascorbate-glutathione cycle (e.g., dehydroascorbic acid and glutathione) also showed significant increases when compared to guard cells treated with elevated CO_2 (**Supplementary Figure S2**).

As to sugars, sugar alcohols and organic acids, which are important for osmoregulation and stomatal opening, most displayed increases under low CO_2, and no changes or decreases under elevated CO_2 (**Supplementary Figure S2**). For example, sucrose and mannitol showed significant increases throughout the low CO_2 treatment, and decreases under elevated CO_2 (**Figure 7**). In pathway enrichment analysis, significantly changed metabolites were enriched in starch and

sucrose metabolism and glycolysis/gluconeogenesis pathways (**Figure 3**). Together with the protein result that significantly changed proteins were overrepresented by the glycolysis pathway (**Figure 7**), we conclude the production of osmolytes to increase guard cell turgor pressure under low CO_2 is mainly from starch breakdown and cellular respiration. Please note that not all the metabolites showed opposite patterns of changes under low CO_2 and elevated CO_2 conditions. For example, malate levels increased under both elevated CO_2 and low CO_2. The sources of malate may be different under these two conditions. Since guard cells have a similar pathway of incorporating CO_2 as C4 photosynthesis (Willmer et al., 1973), it is highly possible that a temporal elevation of CO_2 increases malate through the activities of phosphoenolpyruvate carboxylase and NADP-malate dehydrogenase (Willmer et al., 1973; Asai et al., 2000). The result of malate increase contradicts with previous findings on stomatal closure induced by other stimuli such as darkness (Penfield et al., 2012), elevated CO_2 (Lee et al., 2008) and ABA (Asai et al., 2000). It is possible that malate may not function as an intracellular osmolyte under elevated CO_2 (Geng et al., 2016). While under low CO_2, malate may be imported or produced through starch degradation to function as a major osmolyte and counter ion for K^+ (Santelia and Lawson, 2016).

CONCLUSIONS

Using hyphenated metabolomics and 10-plex TMT based proteomics technologies, we have investigated the metabolomic and proteomic responses of *B. napus* guard cells to low CO_2. A total of 411 metabolites and 1,397 proteins were quantified in this time-course study. Metabolites and proteins that exhibited significant changes are overrepresented in fatty acid metabolism, hormone metabolism, starch and sucrose metabolism, glycolysis and redox regulation. Compared to the previous elevated CO_2 study (Geng et al., 2016), many interesting changes were noted in guard cells under low CO_2. For example, diversion of JA biosynthesis to traumatic acid biosynthesis, the role of melatonin and phytohormone crosstalk, redox regulation and the functions of fatty acid metabolism and Ras-related protein. Future studies focusing on testing the hypotheses generated from this work will greatly enhance our understanding of the molecular mechanisms underlying low CO_2 induced stomatal opening. In addition, as the MS imaging technique moves toward high resolution, *in situ* guard cell metabolomics will be an exciting direction.

AUTHOR CONTRIBUTIONS

SG performed the metabolomics and proteomics experiments, data analysis and paper drafting; BY collected experimental materials and performed proteomics experiments; NZ participated in peptide labeling and data analysis; CD contributed in LC-MS optimization and TMT peptide analysis; and SC designed the experiments, supervised the work and finalized the manuscript. All the authors have read the manuscript and provided comments.

ACKNOWLEDGMENTS

This work has been funded by the US National Science Foundation (NSF) grant 1158000 to SC and partly by a graduate fellowship to SG from the China Scholarship Council. Professor Sally Assmann from the Pennsylvania State University, Dr. Danny Alexander and Dr. Anne M. Evans from Metabolon are acknowledged for invaluable discussions and assistance with methodology. Dr. Qiuying Pang, a visiting scholar from Northeast Forestry University (Harbin, China), helped with data organization. All the proteomics data have been deposited to ProteomeXchange (http://www.proteomexchange.org/) (PXD005787), and the metabolomics data are archived in MetaboLync (https://portal.metabolon.com) (UNFL-03-14VW).

SUPPLEMENTARY MATERIAL

The Supplementary Material for this article can be found online at: http://journal.frontiersin.org/article/10.3389/fmolb.2017.00051/full#supplementary-material

Supplementary Figure S1 | Protein single enrichment analysis of proteins changed in guard cells. **(A)** Biological process; **(B)** Molecular function. The GO terms in the boxes are labeled by GO ID, term definition and statistical information. The significant terms ($p < 0.05$) are marked with color, while non-significant terms are shown as white boxes. Solid, dashed, and dotted lines represent two, one and zero enriched terms at both ends, respectively. The enrichment level is related to the term *p*-values, i.e., the smaller of the term's *p*-value, the more significant statistically, and the node's color is darker and redder. Inside the box of the significant terms, the information includes: GO term, *p*-value, GO description, item number mapping the GO in the query list and background, and total number of query list and background. For those terms with *p*-values > 0.05, only GO information is shown.

Supplementary Figure S2 | Changes of osmoregulators, ROS scavengers, phytohormones and melatonin in guard cells under elevated CO_2 (red) and low CO_2(cyanine blue) conditions. Significant metabolite changes between elevated and low CO_2 treatments ($p < 0.05$) are marked with stars (*).

Supplementary Table S1 | Metabolite information, quantification, mean, fold change, and *p*-value. Identification levels include: (1) Identified compounds; (2) Putatively annotated compounds; (3) Putatively characterized compound classes; (4) Unknown compounds for compound identification levels as recommended by Metabolomics Society's metabolomics standards initiative (MSI).

Supplementary Table S2 | List of all the identified peptides and proteins in the two independent experiments. Highlighted cells indicate proteins with a significance level of $p < 0.05$.

Supplementary Table S3 | List of all the significantly changed proteins (fold change < 0.8 or > 1.2, *p*-value < 0.05) at different time points, with *p*-value and fold change at their corresponding time points.

REFERENCES

Arnao, M. B., and Hernandez-Ruiz, J. (2006). The physiological function of melatonin in plants. *Plant Signal. Behav.* 1, 89–95. doi: 10.4161/psb.1.3.2640

Asai, N., Nakajima, N., Tamaoki, M., Kamada, H., and Kondo, N. (2000). Role of malate synthesis mediated by phosphoenolpyruvate carboxylase in guard cells in the regulation of stomatal movement. *Plant Cell Physiol.* 41, 10–15. doi: 10.1093/pcp/41.1.10

Assmann, S. M. (1999). The cellular basis of guard cell sensing of rising CO_2. *Plant Cell Environ.* 22, 629–637. doi: 10.1046/j.1365-3040.1999.00408.x

Azoulay-Shemer, T., Palomares, A., Bagheri, A., Israelsson-Nordstrom, M., Engineer, C. B., Bargmann, B. O. R., et al. (2015). Guard cell photosynthesis is critical for stomatal turgor production, yet does not directly mediate CO_2- and ABA-induced stomatal closing. *Plant J.* 83, 567–581. doi: 10.1111/tpj.12916

Chalhoub, B., Denoeud, F., Liu, S. Y., Parkin, I. A. P., Tang, H. B., Wang, X. Y., et al. (2014). Early allopolyploid evolution in the post-Neolithic *Brassica napus* oilseed genome. *Science* 345, 950–953. doi: 10.1126/science.1253435

Chen, W., Gong, L., Guo, Z. L., Wang, W. S., Zhang, H. Y., Liu, X. Q., et al. (2013). A novel integrated method for large-scale detection, identification, and quantification of widely targeted metabolites: application in the study of rice metabolomics. *Mol. Plant* 6, 1769–1780. doi: 10.1093/mp/sst080

Chepyshko, H., Lai, C.-P., Huang, L.-M., Liu, J.-H., and Shaw, J.-F. (2012). Multifunctionality and diversity of GDSL esterase/lipase gene family in rice (*Oryza sativa* L. *japonica*) genome: new insights from bioinformatics analysis. *BMC Genomics* 13:309. doi: 10.1186/1471-2164-13-309

Conesa, A., and Götz, S. (2008). Blast2GO: A comprehensive suite for functional analysis in plant genomics. *Int. J. Plant Genomics* 2008:619832. doi: 10.1155/2008/619832

Daloso, D. M., Antunes, W. C., Pinheiro, D. P., Waquim, J. P., Araujo, W. L., Loureiro, M. E., et al. (2015a). Tobacco guard cells fix CO2 by both RubisCO and PEPcase whilst sucrose acts as a substrate during light induced stomatal opening. *Plant Cell Environ.* 38, 2353–2371. doi: 10.1111/pce.12555

Daloso, D. M., Williams, T. C. R., Antunes, W. C., Pinheiro, D. P., Müller, C., Loureiro, M. E., et al. (2015b). Guard cell-specific upregulation of sucrose synthase 3 reveals that the role of sucrose in stomatal function is primarily energetic. *New Phytol.* 209, 1470–1483. doi: 10.1111/nph.13704

Daszkowska-Golec, A., and Szarejko, I. (2013). Open or close the gate - stomata action under the control of phytohormones in drought stress conditions. *Front. Plant Sci.* 4:138. doi: 10.3389/fpls.2013.00138

McLachlan, D. H., Lan, J., Geilfus, C.-M., Dodd, A. N., Larson, T., Baker, A., et al. (2016). The breakdown of stored triacylglycerols is required during light-induced stomatal opening. *Curr. Biol.* 26, 707–712. doi: 10.1016/j.cub.2016.01.019

Du, Z., Zhou, X., Ling, Y., Zhang, Z., and Su, Z. (2010). agriGO: a GO analysis toolkit for the agricultural community. *NAR* 38, W64–W70. doi: 10.1093/nar/gkq310

Engineer, C. B., Ghassemian, M., Anderson, J. C., Peck, S. C., Hu, H., and Schroeder, J. I. (2014). Carbonic anhydrases, EPF2 and a novel protease mediate CO_2 control of stomatal development. *Nature* 513, 246–250. doi: 10.1038/nature13452

Engineer, C. B., Hashimoto-Sugimoto, M., Negi, J., Israelsson-Nordstrom, M., Azoulay-Shemer, T., Rappel, W. J., et al. (2015). CO2 sensing and CO2 regulation of stomatal conductance: advances and open questions. *Trends Plant Sci.* 21, 16–30. doi: 10.1016/j.tplants.2015.08.014

Ephritikhine, G., Fellner, M., Vannini, C., Lapous, D., and Barbier-Brygoo, H. (1999). The sax1 dwarf mutant of Arabidopsis thaliana shows altered sensitivity of growth responses to abscisic acid, auxin, gibberellins and ethylene and is partially rescued by exogenous brassinosteroid. *Plant J.* 18, 303–314. doi: 10.1046/j.1365-313X.1999.00454.x

Evans, A. M., Bridgewater, B. R., Liu, Q., Mitchell, M. W., Robinson, R. J., Dai, H., et al. (2014). High resolution mass spectrometry improves data quantity and quality as compared to unit mass resolution mass spectrometry in high-throughput profiling metabolomics. *Metabolomics* 4:132. doi: 10.4172/2153-0769.1000132

Evans, A. M., Dehaven, C. D., Barrett, T., Mitchell, M., and Milgram, E. (2009). Integrated, nontargeted ultrahigh performance liquid chromatography/electrospray ionization tandem mass spectrometry platform for the identification and relative quantification of the small-molecule complement of biological systems. *Anal. Chem.* 81, 6656–6667. doi: 10.1021/ac901536h

Geng, S., Misra, B. B., Armas, E., Huhman, D., Alborn, H. T., Sumner, L. W., et al. (2016). Jasmonate-mediated stomatal closure under elevated CO_2 revealed by time-resolved metabolomics. *Plant J.* 88, 947–962. doi: 10.1111/tpj.13296

Gish, W. (1996-2009). *AB-BLAST 3.0 Personal Edition*. Available online at: http://blast.advbiocomp.com

Hashimoto, M., Negi, J., Young, J., Israelsson, M., Schroeder, J. I., and Iba, K. (2006). Arabidopsis HT1 kinase controls stomatal movements in response to CO_2. *Nat. Cell Biol.* 8, 391–397. doi: 10.1038/ncb1387

Hastie, T., Tibshirani, R., Narasimhan, B., and Chu, G. (2014). *Impute: Imputation for Microarray Data*. R package version 1.44.40.

Haubrick, L. L., Torsethaugen, G., and Assmann, S. M. (2006). Effect of brassinolide, alone and in concert with abscisic acid, on control of stomatal aperture and potassium currents of *Vicia faba* guard cell protoplasts. *Physiol. Plant.* 128, 134–143. doi: 10.1111/j.1399-3054.2006.00708.x

Holm, L., and Sander, C. (1998). Removing near-neighbour redundancy from large protein sequence collections. *Bioinformatics* 14, 423–429. doi: 10.1093/bioinformatics/14.5.423

Hu, H., Boisson-Dernier, A., Israelsson-Nordstrom, M., Bohmer, M., Xue, S., Ries, A., et al. (2010). Carbonic anhydrases are upstream regulators of CO_2-controlled stomatal movements in guard cells. *Nat. Cell Biol.* 12, 87–93. doi: 10.1038/ncb2009

Hwang, J.-U., Jeon, B. W., Hong, D., and Lee, Y. (2011). Active ROP2 GTPase inhibits ABA- and CO_2-induced stomatal closure. *Plant Cell Environ.* 34, 2172–2182. doi: 10.1111/j.1365-3040.2011.02413.x

Jin, X., Wang, R. S., Zhu, M., Jeon, B. W., Albert, R., Chen, S., et al. (2013). Abscisic acid-responsive guard cell metabolomes of Arabidopsis wild-type and *gpa1* G-protein mutants. *Plant Cell* 25, 4789–4811. doi: 10.1105/tpc.113.119800

Jones, K. A., Kim, P. D., Patel, B. B., Kelsen, S. G., Braverman, A., Swinton, D. J., et al. (2013). Immunodepletion plasma proteomics by tripleTOF 5600 and Orbitrap elite/LTQ-Orbitrap Velos/Q exactive mass spectrometers. *J. Proteome Res.* 12, 4351–4365. doi: 10.1021/pr400307u

Jung, J. Y., Kim, Y. W., Kwak, J. M., Hwang, J. U., Young, J., Schroeder, J. I., et al. (2002). Phosphatidylinositol 3-and 4-phosphate are required for normal stomatal movements. *Plant Cell* 14, 2399–2412. doi: 10.1105/tpc.004143

Kim, S. G., Kim, S. T., Wang, Y., Kim, S.-K., Lee, C. H., Kim, K.-K., et al. (2010). Overexpression of rice isoflavone reductase-like gene *(OsIRL)* confers tolerance to reactive oxygen species. *Physiol. Plant.* 138, 1–9. doi: 10.1111/j.1399-3054.2009.01290.x

Kováts, E. (1958). Gas-chromatographische charakterisierung organischer verbindungen. teil 1: retentionsindices aliphatischer halogenide, alkohole, aldehyde und ketone. *Helv. Chim. Acta* 41, 1915–1932. doi: 10.1002/hlca.19580410703

Lawson, T., Simkin, A. J., Kelly, G., and Granot, D. (2014). Mesophyll photosynthesis and guard cell metabolism impacts on stomatal behaviour. *New Phytol.* 203, 1064–1081. doi: 10.1111/nph.12945

Lawton, K. A., Berger, A., Mitchell, M., Milgram, K. E., Evans, A. M., Guo, L., et al. (2008). Analysis of the adult human plasma metabolome. *Pharmacogenomics* 9, 383–397. doi: 10.2217/14622416.9.4.383

Lee, M., Choi, Y., Burla, B., Kim, Y.-Y., Jeon, B., Maeshima, M., et al. (2008). The ABC transporter AtABCB14 is a malate importer and modulates stomatal response to CO_2. *Nat. Cell Biol.* 10, 1217–1223. doi: 10.1038/ncb1782

Li, C., Tan, D. X., Liang, D., Chang, C., Jia, D. F., and Ma, F. W. (2015). Melatonin mediates the regulation of ABA metabolism, free-radical scavenging, and stomatal behaviour in two Malus species under drought stress. *J. Exp. Bot.* 66, 669–680. doi: 10.1093/jxb/eru476

Liu, X. Q., Li, F., Tang, J. Y., Wang, W. H., Zhang, F. X., Wang, G. D., et al. (2012). Activation of the Jasmonic Acid Pathway by Depletion of the Hydroperoxide Lyase OsHPL3 Reveals Crosstalk between the HPL and AOS Branches of the Oxylipin Pathway in Rice. *PLoS ONE* 7:e50089. doi: 10.1371/journal.pone.0050089

Matrosova, A., Bogireddi, H., Mateo-Penas, A., Hashimoto-Sugimoto, M., Iba, K., Schroeder, J. I., et al. (2015). The HT1 protein kinase is essential for red light-induced stomatal opening and genetically interacts with OST1 in red light and CO_2-induced stomatal movement responses. *New Phytol.* 208, 1126–1137. doi: 10.1111/nph.13566

Medeiros, D. B., Martins, S. C. V., Cavalcanti, J. H. F., Daloso, D. M., Martinoia, E., Nunes-Nesi, A., et al. (2016). Enhanced photosynthesis and growth in *atquac1* knockout mutants are due to altered organic acid accumulation and an increase in both stomatal and mesophyll conductance. *Plant Physiol.* 170, 86–101. doi: 10.1104/pp.15.01053

Meyer, S., Mumm, P., Imes, D., Endler, A., Weder, B., Al-Rasheid, K. A. S., et al. (2010). AtALMT12 represents an R-type anion channel required

for stomatal movement in Arabidopsis guard cells. *Plant J.* 63, 1054–1062. doi: 10.1111/j.1365-313X.2010.04302.x

Misra, B., Acharya, B. R., Granot, D., Assmann, S. M., and Chen, S. (2015). The guard cell metabolome: functions in stomatal movement and global food security. *Front. Plant Sci.* 6:334. doi: 10.3389/fpls.2015.00334

Murashige, T., and Skoog, F. (1962). A revised medium for rapid growth and bio assays with tobacco tissue cultures. *Physiol. Plant.* 15, 473–497. doi: 10.1111/j.1399-3054.1962.tb08052.x

Murata, Y., Mori, I. C., and Munemasa, S. (2015). Diverse stomatal signaling and the signal integration mechanism. *Annu. Rev. Plant Biol.* 66, 369–392. doi: 10.1146/annurev-arplant-043014-114707

Nawaz, M. A., Huang, Y., Bie, Z. L., Ahmed, W., Reiter, R. J., Niu, M. L., et al. (2016). Melatonin: current status and future perspectives in plant science. *Front. Plant Sci.* 6:1230. doi: 10.3389/fpls.2015.01230

Negi, J., Hashimoto-Sugimoto, M., Kusumi, K., and Iba, K. (2014). New approaches to the biology of stomatal guard cells. *Plant Cell Physiol.* 55, 241–250. doi: 10.1093/pcp/pct145

Penfield, S., Clements, S., Bailey, K. J., Gilday, A. D., Leegood, R. C., Gray, J. E., et al. (2012). Expression and manipulation of phosphoenolpyruvate carboxykinase 1 identifies a role for malate metabolism in stomatal closure. *Plant J.* 69, 679–688. doi: 10.1111/j.1365-313X.2011.04822.x

Pharmawati, M., Billington, T., and Gehring, C. A. (1998). Stomatal guard cell responses to kinetin and natriuretic peptides are cGMP-dependent. *Cellular Mol. Life Sci.* 54, 272–276. doi: 10.1007/s000180050149

R Development Core Team (2015). *R: A Language and Environment for Statistical Computing*. Vienna: R Foundation for Statistical Computing.

Roessner-Tunali, U., Hegemann, B., Lytovchenko, A., Carrari, F., Bruedigam, C., Granot, D., et al. (2003). Metabolic profiling of transgenic tomato plants overexpressing hexokinase reveals that the influence of hexose phosphorylation diminishes during fruit development. *Plant Physiol.* 133, 84–99. doi: 10.1104/pp.103.023572

Sakaki, T., Satoh, A., Tanaka, K., Omasa, K., and Shimazaki, K.-I. (1995). Lipids and fatty acids in guard-cell protoplasts from Vicia faba leaves. *Phytochemistry* 40, 1065–1070. doi: 10.1016/0031-9422(95)00272-9

Santelia, D., and Lawson, T. (2016). Rethinking guard cell metabolism. *Plant Physiol.* 172, 1371–1392. doi: 10.1104/pp.16.00767

Schwartz, A., Ilan, N., and Grantz, D. A. (1988). Calcium effects on stomatal movement in *Commelina-Communis L.* - use of EGTA to modulate stomatal response to light, KCl and CO_2. *Plant Physiol.* 87, 583–587. doi: 10.1104/pp.87.3.583

She, X. P., and Song, X. G. (2006). Cytokinin- and auxin-induced stomatal opening is related to the change of nitric oxide levels in guard cells in broad bean. *Physiol. Plant.* 128, 569–579. doi: 10.1111/j.1399-3054.2006.00782.x

Shi, K., Li, X., Zhang, H., Zhang, G., Liu, Y., Zhou, Y., et al. (2015). Guard cell hydrogen peroxide and nitric oxide mediate elevated CO_2 -induced stomatal movement in tomato. *New Phytol.* 208, 342–353. doi: 10.1111/nph.13621

Sierla, M., Waszczak, C., Vahisalu, T., and Kangasjärvi, J. (2016). Reactive oxygen species in the regulation of stomatal movements. *Plant Physiol.* 171, 1569–1580. doi: 10.1104/pp.16.00328

Song, X. G., She, X. P., He, J. M., Huang, C., and Song, T. S. (2006). Cytokinin- and auxin-induced stomatal opening involves a decrease in levels of hydrogen peroxide in guard cells of *Vicia faba*. *Funct. Plant Biol.* 33, 573–583. doi: 10.1071/FP05232

Storey, J. D., Leek, J. T., and Bass, A. J. (2015). *edge: Extraction of Differential Gene Expression.* R package version 2.0.0. Available online at:https://github.com/jdstorey/edge

Tian, W., Hou, C., Ren, Z., Pan, Y., Jia, J., Zhang, H., et al. (2015). A molecular pathway for CO_2 response in Arabidopsis guard cells. *Nat. Commun.* 6:6057. doi: 10.1038/ncomms7057

Wang, C., Hu, H., Qin, X., Zeise, B., Xu, D., Rappel, W. J., et al. (2016). Reconstitution of CO_2 Regulation of SLAC1 Anion Channel and Function of CO_2-Permeable PIP2;1 Aquaporin as CARBONIC ANHYDRASE4 Interactor. *Plant Cell* 28, 568–582. doi: 10.1105/tpc.15.00637

Watkins, J. M., Hechler, P. J., and Muday, G. K. (2014). Ethylene-induced flavonol accumulation in guard cells suppresses reactive oxygen species and moderates stomatal aperture. *Plant Physiol.* 164, 1707–1717. doi: 10.1104/pp.113.233528

Webb, A. A. R., McAinsh, M. R., Mansfield, T. A., and Hetherington, A. M. (1996). Carbon dioxide induces increases in guard cell cytosolic free calcium. *Plant J.* 9, 297–304. doi: 10.1046/j.1365-313X.1996.09030297.x

Willmer, C. M., Grammatikopoulos, G., LascÈve, G., and Vavasseur, A. (1995). Characterization of the vacuolar-type H^+-ATPase from guard cell protoplasts of Commelina. *J. Exp. Bot.* 46, 383–389. doi: 10.1093/jxb/46.4.383

Willmer, C. M., Pallas, J. E., and Black, C. C. (1973). Carbon dioxide metabolism in leaf epidermal tissue. *Plant Physiol.* 52, 448–452. doi: 10.1104/pp.52.5.448

Xia, J., Sinelnikov, I. V., Han, B., and Wishart, D. S. (2015). MetaboAnalyst 3.0-making metabolomics more meaningful. *NAR* 43, W251–W257. doi: 10.1093/nar/gkv380

Xu, H. L., Shida, A., Futatsuya, F., and Kumura, A. (1994a). Effects of Epibrassinolide and Abscisic-Acid on Sorghum Plants Growing under Soil-Water Deficit.1. Effects on Growth and Survival. *Jpn. J. Crop Sci.* 63, 671–675. doi: 10.1626/jcs.63.671

Xu, H. L., Shida, A., Futatsuya, F., and Kumura, A. (1994b). Effects of Epibrassinolide and Abscisic-Acid on Sorghum Plants Growing under Soil-Water Deficit.2. Physiological-Basis for Drought Resistance Induced by Exogenous Epibrassinolide and Abscisic-Acid. *Jpn. J. Crop Sci.* 63, 676–681. doi: 10.1626/jcs.63.676

Xue, S., Hu, H., Ries, A., Merilo, E., Kollist, H., and Schroeder, J. I. (2011). Central functions of bicarbonate in S-type anion channel activation and OST1 protein kinase in CO_2 signal transduction in guard cell. *EMBO J.* 30, 1645–1658. doi: 10.1038/emboj.2011.68

Young, J. J., Mehta, S., Israelsson, M., Godoski, J., Grill, E., and Schroeder, J. I. (2006). CO_2 signaling in guard cells: calcium sensitivity response modulation, a Ca^{2+}-independent phase, and CO_2 insensitivity of the *gca2* mutant. *Proc. Natl. Acad. Sci. U.S.A.* 103, 7506–7511. doi: 10.1073/pnas.0602225103

Zeiger, E., and Zhu, J. X. (1998). Role of zeaxanthin in blue light photoreception and the modulation of light-CO_2 interactions in guard cells. *J. Exp. Bot.* 49, 433–442. doi: 10.1093/jxb/49.Special_Issue.433

Zhang, Y., Zhu, H., Zhang, Q., Li, M., Yan, M., Wang, R., et al. (2009). Phospholipase Dα1 and Phosphatidic Acid Regulate NADPH Oxidase Activity and Production of Reactive Oxygen Species in ABA-Mediated Stomatal Closure in Arabidopsis. *Plant Cell* 21, 2357–2377. doi: 10.1105/tpc.108.062992

Zhu, C. M., and Yoshikawa-Inoue, H. (2015). Seven years of observational atmospheric CO_2 at a maritime site in northernmost Japan and its implications. *Sci. Total Environ.* 524–525, 331–337. doi: 10.1016/j.scitotenv.2015.04.044

Zhu, J., Talbott, L. D., Jin, X., and Zeiger, E. (1998). The stomatal response to CO_2 is linked to changes in guard cell zeaxanthin. *Plant Cell Environ.* 21, 813–820. doi: 10.1046/j.1365-3040.1998.00323.x

Zhu, M., Dai, S., Zhu, N., Booy, A., Simons, B., Yi, S., et al. (2012). Methyl jasmonate responsive proteins in *Brassica napus* guard cells revealed by iTRAQ-based quantitative proteomics. *J. Proteome Res.* 11, 3728–3742. doi: 10.1021/pr300213k

Zhu, M., Simons, B., Zhu, N., Oppenheimer, D. G., and Chen, S. (2010). Analysis of abscisic acid responsive proteins in *Brassica napus* guard cells by multiplexed isobaric tagging. *J. Proteomics* 73, 790–805. doi: 10.1016/j.jprot.2009.11.002

Conflict of Interest Statement: CD is associated with Thermo Scientific Inc., and there is no conflict of interest in this basic research. CD contributed in LC-MS optimization for achieving optimal resolving power of the 10-plex TMT tagged peptides and acquired the LC-MS data of the TMT peptides that used to identify the low CO_2 responsive proteins in this study.

The other authors declare that the research was conducted in the absence of any commercial or financial relationships that could be construed as a potential conflict of interest.